Journal of Alloys and Compounds 491 (2010) 595–598

Contents lists available at ScienceDirect

Journal of Alloys and Compounds

journal homepage: www.elsevier.com/locate/jallcom

Temperature dependence of photoluminescence from as-grown and plasma-etched $InAs_{0.45}P_{0.55}/In_{0.68}Ga_{0.32}As_{0.45}P_{0.55}$ strained single quantum well

Meng Cao[a,b,*], Hui-Zhen Wu[b], Yan-Feng Lao[b], Chun-Fang Cao[b], Cheng Liu[b], Gu-Jin Hu[a]

[a] National Laboratory of Infrared Physics, Shanghai Institute of Technical Physics, Chinese Academy of Sciences, Shanghai 200083, China
[b] State Key Laboratory of Functional Materials for Informatics, Shanghai Institute of Microsystem and Information Technology, Chinese Academy of Sciences, Shanghai 200050, China

ARTICLE INFO

Article history:
Received 7 May 2009
Received in revised form 29 October 2009
Accepted 3 November 2009
Available online 11 November 2009

Keywords:
Quantum well
Etching
Photoluminescence

ABSTRACT

The temperature and laser pumping power dependent photoluminescence (PL) has been investigated on strained single quantum wells (SSQWs) using inductively coupled-plasma (ICP) etching method. Significant improvement of PL performances was observed in the plasma-etched SSQW in comparison with the as-grown samples. The enhancement factor increases with the increasing of temperature, but decreases with the increasing of pump power. At lower temperatures, the larger full width at half maximum (FWHM) and the blue-shift of PL peak positions for the plasma-etched SSQW may be attributed to the damage and reduced composition fluctuation within the quantum well structure aroused during plasma etching.

1. Introduction

With the growing reduction in dimensions of optoelectronic devices, low damage and anisotropic etching processes, such as ICP, are highly desirable for device patterning [1–4]. Even though ICP-introduced structural damage may exist in semiconductors, tremendous efforts have been devoted to minimized or recovery the damage [5,6]. The performance of some optoelectronic devices such as light emitting diodes (LEDs) can even be enhanced due to the improved light extraction efficiency after ICP etching [7,8]. And greatly enhanced optical properties of plasma-treated group III–V quantum wells (QWs) or group II–VI nanorods were also reported in previous work [9,10]. But the PL properties of plasma-etched group III–V QWs influenced by temperature and laser pumping power are still not well studied.

In this letter, an obviously enhanced PL intensity of $InAs_{0.45}P_{0.55}/In_{0.68}Ga_{0.32}As_{0.45}P_{0.55}$ strained single quantum well (SSQW) after plasma etching was observed in our experiments. The enhancement factor is greatly influenced by temperature and pumping power. This abnormal phenomenon promotes us to explore the difference of the PL properties between the as-grown and plasma-etched $InAs_{0.45}P_{0.55}/In_{0.68}Ga_{0.32}As_{0.45}P_{0.55}$ SSQW changed with temperature and pump power.

2. Experimental details

$InAs_{0.45}P_{0.55}/In_{0.68}Ga_{0.32}As_{0.45}P_{0.55}$ SSQW were grown on InP (100) semi-insulating substrate by Thermal V90 gas-source molecule-beam epitaxy (GSMBE) [11]. A 50 nm InP buffer layer was grown on substrate first. A single quantum well comprising two 10 nm $In_{0.68}Ga_{0.32}As_{0.45}P_{0.55}$ barrier layer and a 9 nm $InAs_{0.45}P_{0.55}$ well layer ($\Delta E_c = 0.14$ eV, $\Delta E_v = 0.05$ eV) was then followed. A 50 nm InP cap layer was covered finally. Before plasma etching, one half of the sample surface was deposited with 420 nm SiN_x by plasma-enhancement chemical-vapor deposit (PECVD). The samples were then etched to different depths by inductively coupled-plasma-98C (ICP-98C). The etching-gases used in ICP were Cl_2 and Ar with flow rates of 6 and 12 sccm, respectively. The ICP power was 200 W with an auto bias of 130 V. The times for ICP etching to etch 10-nm InP, 20-nm InP and 40-nm InP are 15, 21 and 28 s, respectively. After plasma etching, SiN_x was removed by diluted HF solution (1:10). Diluted HF solution etches alloys with high contents of AlAs and AlSb, but not those with high contents of GaAs, InAs, and InP, so it does not damage the QW structure [12]. The etching depth was measured by a Talystep profiler (XP-2) and the typical intrinsic error of the Talystep profiler is 3.7 nm. Roughness of mean square (RMS) of the surface of the as-grown and ICP-etched sample is 0.52 and 1.98 nm recorded by the Talystep profiler. The QW PL spectra were measured by Fourier transform infrared (FTIR) photoluminescence experimental system (Nicolet-760). The 514.5-nm line of an Ar^+ laser was used for excitation. Samples were mounted in a cryostat using gases He as a refrigerating medium. The temperature of samples was controlled within the accuracy of ±0.1 K using a temperature controller.

3. Results and discussion

Fig. 1 shows the PL spectra of the as-grown and plasma-etched $In_{0.68}Ga_{0.32}As_{0.45}P_{0.55}$ SSQW at 10 K. It can be seen that the SSQW PL peak intensity increases gradually when the etching depth is smaller than 40 nm, and then quickly decreases with further increasing of the etching depth. The PL peak wavelength of the plasma-etched samples exhibit a blue-shift compared with that of the as-grown sample can be ascribed to composition fluctuation

* Corresponding author at: National Laboratory of Infrared Physics, Shanghai Institute of Technical Physics, Chinese Academy of Sciences, 500 YuTian RD, Shanghai 200083, China. Tel.: +86 21 65420850x24411; fax: +86 21 65830734.
E-mail address: caomeng_0107@163.com (M. Cao).

0925-8388/$ – see front matter © 2009 Elsevier B.V. All rights reserved.
doi:10.1016/j.jallcom.2009.11.014

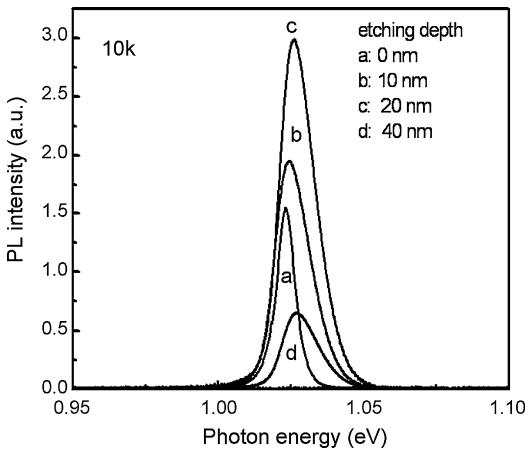

Fig. 1. PL spectra of an $InAs_{0.45}P_{0.55}/In_{0.68}Ga_{0.32}As_{0.45}P_{0.55}$ SSQW at low temperature 10 K for different etching depths.

and strain change inside the QWs structures which will be detailedly discussed in the following part [13,14]. The increased PL intensity can be understood by considering the following facts: (a) plasma etching process induces surface roughness, which is known to enhance light extraction efficiency of QW; (b) molecular dynamics simulations show that Ar^+ ions have the nonzero diffusion probability along ⟨1 1 0⟩ direction on III–V semiconductors even with low energies [15]. Therefore, a portion of incoming Ar^+ ions (∼0.1%) penetrates into the QW, which partially passivates the grown-in defects within the strained QW structures [16,17]; (c) The thinner capping layer allow more pumping light be absorbed by QW. However, a longer etching time will introduce much more Ar^+ ions in the QW structure not only damaging the QW structure but acting as defects, ultimately leading to a degradation of PL intensity.

Fig. 2 indicates PL spectra of the as-grown and plasma-etched $InAs_{0.45}P_{0.55}/In_{0.68}Ga_{0.32}As_{0.45}P_{0.55}$ SSQW at various temperatures between 20 and 300 K under a constant pumping power of 30 mW. The PL peaks continually shifts toward the high photo-energy side with the narrowing of the line-width when temperatures are decreased. The PL enhancement factor Q which is defined as the ratio of peak intensity of etched sample to the as-grown one, increases with the rising of temperature but decreases with the pumping power, as shown in the inset of Fig. 2(b). As radiative and nonradiative recombination coexists during an external exciting irradiation, their competition determines the temperature dependent PL behavior as to InAsP/InGaAsP QW system, the photogenerated carriers contributing to nonradiative recombination dominates at higher temperatures, whereas radiative excitons recombination at lower temperatures [18,19]. Composition fluctuation, well-width fluctuation and interface roughness could exist inside the as-grown QW structure. These grow-in structural variations lead to an effective band-gap modulation in the growth direction and a statistical distribution of local potential minima [20]. At low temperatures, the minima act as trap sites and the photogenerated excitons in the wells can drift towards the potential minima as the drift time is much shorter than that they are captured by nonradiative centers [21]. Therefore, the internal quantum efficiency of the as-grown sample increases at low temperatures and closes to that of the etched sample due to the low capture rate of the excitons. But at high temperatures, excitons can escape from the potential minima by thermal excitation and hence carriers could be mostly captured by nonradiative recombination centers inside the as-grown sample which leads to a decreased internal quantum efficiency. But there are less grown-in defects inside the etched sample due to passivation of appropriate Ar^+ ions dwelling in. So the internal quantum efficiency of the as-grown sample

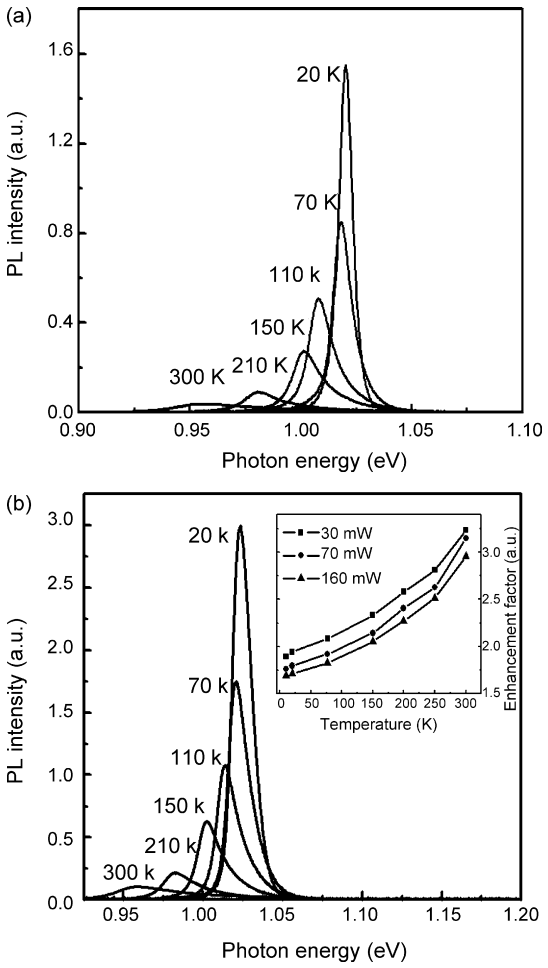

Fig. 2. PL spectra of an $InAs_{0.45}P_{0.55}/In_{0.68}Ga_{0.32}As_{0.45}P_{0.55}$ SSQW at different temperatures with a constant pumping power (30 mW) for (a) as-grown sample and (b) plasma-etched 20 nm sample. In the inset of Fig. 2(b) shows the PL intensity enhancement factor of plasma-etched sample versus temperature for different pumping power.

decreases more rapidly than that of the plasma-etched sample giving an increased PL enhancement factor at high temperatures. At a given temperature, more free carriers will be produced in the $InAs_{0.45}P_{0.55}/In_{0.68}Ga_{0.32}As_{0.45}P_{0.55}$ SSQW under a higher optical pumping power. And the free carriers can screen the potential minima and weaken the emission of light, resulting in a small value of Q in the plasma-etched sample.

Fig. 3 indicates the PL intensities variation of both samples for different pumping power at three different temperatures. At a certain temperature, the PL intensities of both the plasma-etched and as-grown samples increase almost linearly with the pumping power. The PL intensities, however, increase relatively slow when the pumping power is high at low temperatures, especially at 10 K. This can be attributed to the excitons screening effect [22]. At very low temperatures, the exciton screening effect is predominant over the intensity dependence of the excitonic relative population under a higher excitation, resulting in a reduced PL increase rate [19]. When temperatures increase, the excitons screening effect does not exist as the phonons relax the binding energy of the excitons, then the rate of PL intensity enhancement accelerates with the increasing of pump power.

Fig. 4 shows the relation of PL peak energy of $InAs_{0.45}P_{0.55}/In_{0.68}Ga_{0.32}As_{0.45}P_{0.55}$ SSQW with temperatures. The temperature dependence of PL peak energy of $InAs_{0.45}P_{0.55}/In_{0.68}Ga_{0.32}As_{0.45}P_{0.55}$ SSQW can be expressed by

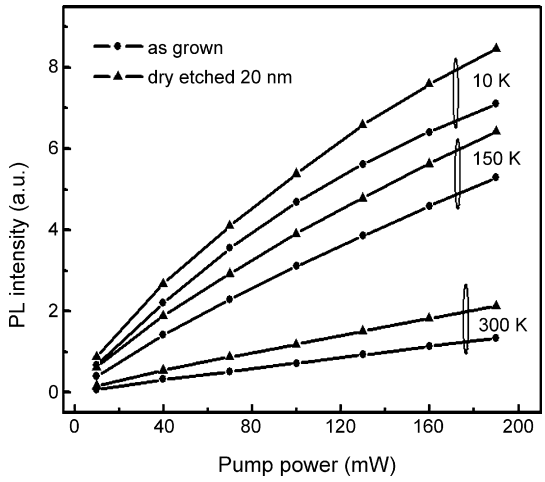

Fig. 3. PL intensity of an $InAs_{0.45}P_{0.55}/In_{0.68}Ga_{0.32}As_{0.45}P_{0.55}$ SSQW versus pumping power at different temperatures.

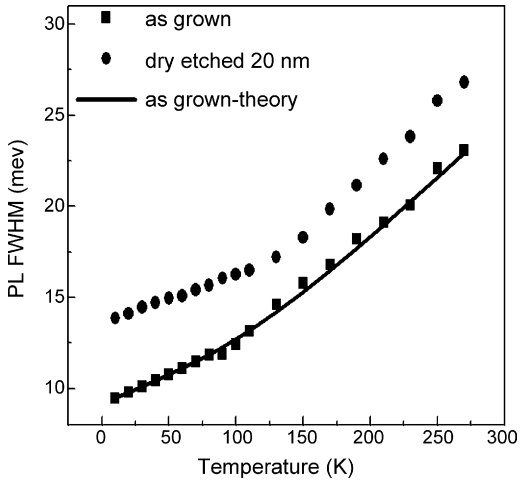

Fig. 5. PL FWHM of an $InAs_{0.45}P_{0.55}/In_{0.68}Ga_{0.32}As_{0.45}P_{0.55}$ SSQW before and after plasma etching versus temperature. The solid line is a fitting curve for the as-grown sample based on the exciton-photon coupling model.

Varshni equation [23]:

$$E_g(T) = E_g(0) - \frac{\alpha T^2}{T+\beta} \quad (1)$$

$E_g(0)$ is the energy gap at 0 K, the fitted α, β, are material parameters. The PL peak energies of both samples shift to the lower energies side with the increasing of temperature. Compared with the as-grown samples, the PL peak energy of the plasma-etched samples shift to the higher energies. And their difference becomes distinct at low temperatures. As there are more composition fluctuation, well-width fluctuation and interface roughness inside the as-grown sample which give rise to a statistical distribution of local potential minima, hence PL emission lies at the lower energy [24,25]. The etching process could have a homogenizing effect on these composition fluctuation and interface roughness. So the PL peaks of the plasma-etched sample shift to the higher energy. The coincidence of the PL peaks of the as-grown sample with that of etched ones at higher temperatures is due to the escape of carriers over the potential minima by thermal excitation.

The overall temperature dependence of the luminescence efficiencies of the as-grown and plasma-etched sample is shown in the inset of Fig. 4. It can be seen that, at low temperatures, the luminescence efficiency of the localized excitons will be very high, most probably ~100%. This will be due to the lower capture rate of the localized excitons by the nonradiative recombination sites compared to that of freely movable excitons. At high temperatures, the carriers can escape from the localized regions through thermal excitation; therefore the PL peak of the as-grown sample starts to coincide with that of the plasma-etched sample [26]. It can also be seen that, the temperature range in which the luminescence efficiency begins to decrease shows good consistence with the temperature range of thermal activation of the localized excitons.

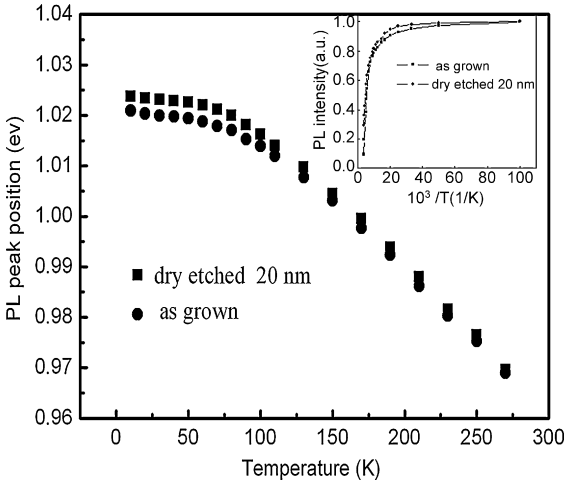

Fig. 4. PL peak energy of $InAs_{0.45}P_{0.55}/In_{0.68}Ga_{0.32}As_{0.45}P_{0.55}$ SSQW before and after plasma etching versus temperature. The inset shows the integrated PL intensity of $InAs_{0.45}P_{0.55}/In_{0.68}Ga_{0.32}As_{0.45}P_{0.55}$ SSQW before and after plasma etching versus temperature.

Fig. 5 shows the variations of PL FWHM as a function of temperature for both as-grown and plasma-etched $InAs_{0.45}P_{0.55}/In_{0.68}Ga_{0.32}As_{0.45}P_{0.55}$ SSQW. The temperature dependent FWHM of the $InAs_{0.45}P_{0.55}/In_{0.68}Ga_{0.32}As_{0.45}P_{0.55}$ SQW as-grown sample can be well fitted to the exciton-photon coupling model [27]:

$$\Gamma(T) = \Gamma_i + \Gamma_a T + \frac{\Gamma_b}{\exp(E_{LO}/k_B T) - 1} \quad (2)$$

where Γ_i is inhomogeneous part, and Γ_a, Γ_b represent the corresponding coupling strengths with acoustic and longitudinal optical (LO) phonon, respectively. E_{LO} is the energy of LO phonon, and k_B is the Boltzmann constant. For $InAs_{0.45}P_{0.55}/In_{0.68}Ga_{0.32}As_{0.45}P_{0.55}$ SSQW, the values for Γ_i, Γ_a, Γ_b, E_{LO} are 7.21 meV, 0.03 meV/K, 17.1 and 36.1 meV, respectively. The PL FWHM of plasma-etched sample is obviously wider than that of the as-grown sample, especially when the temperature is below 70 K. In general, the luminescence line shape is a convolution of an inhomogeneous part and a temperature dependent homogeneous part. Interface roughness and random alloy disorder mainly contribute to the inhomogeneous line-width in the strained quantum well structure, especially in the low-temperature range [28]. There is more alloy disorder inside plasma-etched samples compared to as-grown samples. Thus its inhomogeneous broadening is larger than that of as-grown sample. At higher temperatures, the contribution of longitudinal optical photons to the homogeneous part of the line-width broadening becomes dominant due to the increasing of photon population, which has almost the same effect on both types of samples [29]. So the FWHM different between the plasma-etched and as-grown sample is reduced.

4. Conclusions

Temperature dependence of PL spectra for plasma-etched and as-grown $InAs_{0.45}P_{0.55}/In_{0.68}Ga_{0.32}As_{0.45}P_{0.55}$ SSQW was measured in the temperature range of 10–300 K. Significant enhancement of PL intensity was achieved for the plasma-etched sample compared with that of the as-grown sample. This is due to the surface roughening and microstructure transformation triggered by Ar^+ ions channeling into the QW structure. The PL enhancement factor increases with the temperature. A larger FWHM and PL intensity peak position blue-shift of the plasma-etched sample were also observed. This is due to the strain damage and reduced composition fluctuation inside the QW structure during the plasma process.

Acknowledgements

The authors thank the support of the National Key Basic Research and Development Program of China (Grant No. 2003CB314903), National Natural Science Foundation of China (Grants No. 60578058 and 10774154), the Knowledge Innovation Program of the Chinese Academy of Sciences, and Shanghai City Committee of Science and Technology in China (Grants No. 07JC14058, 08JC1420900, and 0752nm016).

References

[1] J.X. Wang, P.Q. Gao, M. Yin, Y.L. Qin, H.Q. Yan, J.S. Li, S.L. Peng, D.Y. He, J. Alloys Compd. 481 (2009) 278.
[2] D.K. Xu, W.N. Tang, L. Liu, Y.B. Xu, E.H. Han, J. Alloys Compd. 432 (2007) 129.
[3] R. Hostein, A. Michon, G. Beaudoin, N. Gogneau, G. Patriache, J.Y. Marzin, I. Robert-Philip, I. Sagnes, A. Beveratos, Appl. Phys. Lett. 93 (2008) 073106.
[4] K. Abedi, V. Ahmadi, E. Darabi, M.K. Moravvej Farshi, M.H. Sheikhi, Solid State Electron. 52 (2008) 312.
[5] S.J. An, J.H. Chae, G.C. Yi, G.H. Park, Appl. Phys. Lett. 92 (2008) 121108.
[6] M.K. Kwon, J.Y. Kim, I.K. Park, K.S. Kim, G.Y. Jung, S.J. Park, Appl. Phys. Lett. 92 (2008) 251110.
[7] H.Y. Gao, F.W. Yan, Y. Zhang, J.M. Li, Y.P. Zeng, G.H. Wang, Solid State Electron. 52 (2008) 962.
[8] H.W. Huang, C.H. Lin, C.C. Yu, B.D. Lee, C.H. Chiu, C.F. Lai, H.C. Kuo, K.M. Leung, T.C. Lu, S.C. Wang, Nanotechnology 19 (2008) 185301.
[9] L.H. Quang, C.S. Jin, J. Electrochem. Soc. 155 (2008) K105.
[10] M. Cao, Y.F. Lao, H.Z. Wu, C. Liu, J. Vac. Sci. Technol. A 26 (2008) 219.
[11] Z.C. Huang, H.Z. Wu, Y.F. Lao, M. Cao, C. Liu, J. Cryst. Growth 281 (2005) 255.
[12] K. Hjort, J. Micromech, Microengineering 6 (1996) 370.
[13] S.J. Xu, X.C. Wang, S.J. Chua, Appl. Phys. Lett 72 (1998) 3335.
[14] S.J. Xu, X.C. Wang, S.J. Chua, Appl. Phys. Lett 77 (2000) 2130.
[15] K. Gärtner, D. Stock, C. Wende, M. Nitschke, Nucl. Instrum. Methods Phys. Res. B 90 (1994) 124.
[16] N.G. Stoffel, J. Vac. Sci. Technol. B 10 (1992) 651.
[17] H.S. Djie, T. Mei, J. Arokiaraj, Appl. Phys. Lett. 83 (2003) 60.
[18] Y.G. Zhao, R.A. Masut, J.L. Brebner, J.T. Graham, J. Appl. Phys. 76 (1994) 5921.
[19] M. Colocci, M. Gurioli, A. Vinattieri, J. Appl. Phys. 68 (1990) 2809.
[20] H.W. Yoon, D.R. Wake, J.P. Wolfe, Phys. Rev. B 54 (1996) 2763.
[21] C. Delalande, M.H. Meynadier, M. Voos, Phys. Rev. B 31 (1985) 2497.
[22] S.R. Jin, Y.L. Zheng, A.Z. Li, J. Appl. Phys. 82 (1997) 3870.
[23] S.R. Jin, A.Z. Li, J. Appl. Phys. 81 (1997) 7357.
[24] M.L. Dotor, M. Recio, D. Golmayo, F. Briones, J. Appl. Phys. 72 (1992) 5861.
[25] D.S. Jiang, H. Jung, K. Ploog, J. Appl. Phys. 64 (1988) 1371.
[26] H. Nashiki, I. Suemune, H. Suzuki, K. Uesugi, Jpn. J. Appl. Phys. Part 1 36 (1997) 4199.
[27] T. Takeuchi, S. Sota, M. Katsuragawa, M. Komori, Jpn. J. Appl. Phys. Part 2 6 (1997) L382.
[28] C.Y. Lee, M.C. Wu, H.P. Shao, W.J. Ho, J. Cryst. Growth 208 (2000) 137.
[29] W.Z. Shen, Y. Chang, S.C. Shen, W.G. Tang, Y. Zhao, A.Z. Li, J. Appl. Phys. 79 (1996) 2139.